

Available online at [www.sciencedirect.com](http://www.sciencedirect.com)

ScienceDirect

journal homepage: [www.elsevier.com/locate/ije](http://www.elsevier.com/locate/ije)

# Modelling of fast fueling of pressurized hydrogen tanks for maritime applications

Netaji Ravikiran Kesana<sup>a</sup>, Prasanna Welahettige<sup>b</sup>, Per Morten Hansen<sup>b</sup>, Øystein Ulleberg<sup>a,\*</sup>, Knut Vågsæther<sup>b</sup>

<sup>a</sup> Institute for Energy Technology, P.O. Box 40, NO-2027, Kjeller, Norway

<sup>b</sup> Department of Process, Energy and Environmental Technology, University of South-Eastern Norway, Kjølnes Ring 56, 3918, Porsgrunn, Norway

## HIGHLIGHTS

- Modeling of gas temperature development inside hydrogen tanks during pressurization.
- Inhomogeneous gas temperature distribution occurs inside large hydrogen tanks.
- Important to understand how heat transfer in tank wall affects heating of the gas.
- Monitoring of the gas temperature at the end of large tanks is recommended.

## ARTICLE INFO

### Article history:

Received 6 January 2023

Received in revised form

10 April 2023

Accepted 13 April 2023

Available online 6 May 2023

### Keywords:

Pressurized hydrogen tanks

Hydrogen fast filling

CFD modeling

Heat transfer

Maritime applications

## ABSTRACT

This paper studies fast fueling of gaseous hydrogen into large hydrogen (H<sub>2</sub>) tanks suitable for maritime applications. Three modeling methods have been developed and evaluated: (1) Two-dimensional computational fluid dynamic (CFD) modeling, (2) One-dimensional wall discretized modeling, and (3) Zero-dimensional modeling. A detailed 2D CFD simulation of a small H<sub>2</sub>-tank was performed and validated with data from literature and then used to simulate a large H<sub>2</sub>-tank. Results from the 2D-model show non-uniform temperature distribution inside the large tank, but not in the small H<sub>2</sub>-tank. The 1D-model can predict the mean temperature in small H<sub>2</sub>-tanks, but not the inhomogeneous temperature field in large H<sub>2</sub>-tanks. The 0D-model is suitable as a screening tool to obtain rough estimates. Results from the modeling of the large H<sub>2</sub>-tank show that the heat transfer to the wall during fast filling is inhibited by heat conduction in the wall which leads to an unacceptably high mean hydrogen temperature.

© 2023 The Authors. Published by Elsevier Ltd on behalf of Hydrogen Energy Publications LLC. This is an open access article under the CC BY license (<http://creativecommons.org/licenses/by/4.0/>).

## Introduction

Hydrogen (H<sub>2</sub>) is a promising alternative fuel for short-range and near-coastal maritime transport operations, such as ferries, supply ships, and bulk transport carriers. However, if

these maritime vessels are to be operated on gaseous hydrogen it will be necessary to store pressurized hydrogen in H<sub>2</sub>-tanks that are much larger than those typically used in fuel cell vehicles. Furthermore, fast fueling of large H<sub>2</sub>-tanks will (similarly to smaller H<sub>2</sub>-tanks) be limited by the maximum

\* Corresponding author.

E-mail address: [oystein.ulleberg@ife.no](mailto:oystein.ulleberg@ife.no) (Ø. Ulleberg).

<https://doi.org/10.1016/j.ijhydene.2023.04.142>

0360-3199/© 2023 The Authors. Published by Elsevier Ltd on behalf of Hydrogen Energy Publications LLC. This is an open access article under the CC BY license (<http://creativecommons.org/licenses/by/4.0/>).

possible temperature increase in the H<sub>2</sub>-tank during fast refueling. It is, therefore, necessary to study this in more detail.

The H<sub>2</sub>-tank wall material properties determine the operating temperature limit. The temperature rise can take place due to the following: (1) Dispenser throttling work (comparatively small) [1], (2) Conversion of kinetic energy into internal energy, and/or (3) Compression of the gas inside the tank caused by the inflow of high-pressure gas [2]. Suryan et al. [3] showed in a CFD study that the flow velocity gradually decreases with an increase in pressure as the density of gas increases during tank filling. Bourgeois et al. [4] showed that the convective heat transfer coefficient between gas and the tank's inner surface gradually changes while filling. Inhomogeneous temperature distribution can occur in the tank, such as thermal stratification. Melideo et al. [5] showed that there can be colder regions due to jet expansions and that the difference between the coldest and hottest regions in the tanks can be up to 30 °C. Johnson et al. [6] investigated the buoyancy effect, which can influence the uneven temperature distribution in the inner surface wall of the tank. A CFD study made by Kim et al. [7] showed that the upper gas temperature is higher than the lower gas temperature due to the buoyancy effect. There are also other studies on the filling of smaller (fuel cell vehicle size) pressurized hydrogen tanks [8–10].

Standard hydrogen pressure vessels (i.e., H<sub>2</sub>-tanks) for fuel cell vehicles and buses have a volume of 50–150 L [11,12]. However, there is limited knowledge on the refueling of large H<sub>2</sub>-tanks that would be suitable for use in maritime applications. The fluid dynamics associated with the H<sub>2</sub>-tank refueling will depend on the H<sub>2</sub>-tank size. A small H<sub>2</sub>-tank for a light-duty fuel cell vehicle or a bus typically contains 2–5 kg of hydrogen (@ 350–700 bar) while large H<sub>2</sub>-tanks suitable for distribution of gaseous hydrogen and storage systems in maritime applications typically will have a capacity of about 30–40 kg (@ 200–350 bar). The lengths of the pressurized gas hydrogen storage tanks can vary from 1 to 2 m in small tanks to 5–6 m in large H<sub>2</sub>-tanks. The jet formation in the H<sub>2</sub>-tanks occurs in the longitudinal direction. This means that the fluid dynamic behavior inside a large and long H<sub>2</sub>-tank will be very different to that in a small and short H<sub>2</sub>-tank.

This study focuses on the modeling and numerical analysis of the fast fueling of large H<sub>2</sub>-tanks. A key objective with the study was to assess the need for detailed and complex computational fluid dynamic (CFD) H<sub>2</sub>-tank simulations in the modeling of hydrogen refueling processes and to investigate how simplified non-dimensional H<sub>2</sub>-tank models can be used in more high-level hydrogen refueling system models. Hence, three types of modeling and simulation methods with different degrees of complexity and areas of application were developed, analyzed, and validated in this study.

## Model description

The three modeling methods developed and evaluated in this study were based on: (1) Two-dimensional (2D) CFD-modeling, (2) One-dimensional (1D) wall discretized modeling, and (3) Zero-dimensional (0D) modeling. The main goal of the modeling in all the three cases is to predict the temperature

and pressure increase inside a H<sub>2</sub>-tank during a refueling process. In the detailed 2D CFD-model the temperature field is computed for both solid and fluid computational zones, while in the 1D and 0D models no fluid dynamics effects are accounted for. In the 1D-model the heat transfer through the tank wall is based on a 1D discretization of the wall and temperature distribution through the wall, while in the 0D-model there is a more simplified approach for estimating the heat transfer. More details on the three different modeling approaches are provided in sections below.

### Two-dimensional CFD model

A transient CFD-analysis was performed for the filling of a compressed H<sub>2</sub>-tank. Two detailed 2D CFD simulations were conducted as a part of this study. The purpose of the first simulation (Case 1) was to validate the CFD-model using data found in the literature. The CFD-results were then compared to experimental data extracted from Dicken and Mérida [13], who performed temperature measurements inside a 74-L tank using thermocouples during the H<sub>2</sub>-filling process. The validated CFD-model was then applied in a simulation study of a large H<sub>2</sub>-tank (Case 2), where a fast H<sub>2</sub>-refueling rate (ca. 1 kg/min) was assumed. The results obtained on flow and temperature fields inside the large H<sub>2</sub>-tank were then analyzed.

#### Case 1: 2D CFD simulation of small H<sub>2</sub>-tank (validation case)

The calculation domain for the 2D CFD-model used in Case 1 of this study is shown in Fig. 1. The fluid flows into the tank from a 5 mm nozzle. The nozzle is protruded 82 mm into the tank. The solid materials (liner with a thickness of 4 mm and laminate of 15 mm) are included in the model. The dimensions of the H<sub>2</sub>-tank are represented accordingly. An overview of the materials and additional details about the geometry and operating procedure used in the experiments can be found in Dicken and Mérida [13]. It should be noted here that axisymmetric boundary conditions have been applied during the simulation, but for the sake of clarity, only 2D geometry images are shown.

The Ansys-Fluent 2020 R1 solver package was used for the analyses. Transient simulations were performed and the system of coupled governing equations solved included continuity, momentum, turbulence, and energy equations. Expressions of these solved equations are presented in many classical fluid mechanics textbooks. The Fluent user manual provides more detailed information regarding the mathematical nature of the equations in this study. A summary of the parameters used for the Case 1 simulation study is presented in Table 1.

The computational mesh used for the analysis in Case 1 is presented in Fig. 2. The mesh consists of quadrilateral and triangular elements, while the solid materials and the nozzle were modeled using only quadrilateral elements. The smallest element size is 0.1 mm and the largest element is 1 mm. The small elements were placed very close to the nozzle where large velocity gradients can be expected due to the turbulent jet propagation into the tank interior volume. In the 2D CFD-modeling of the small H<sub>2</sub>-tank (Case 1) approximately 20,000 computational cells were used in the simulation, with cell sizes ranging from 1 mm to 5 mm.

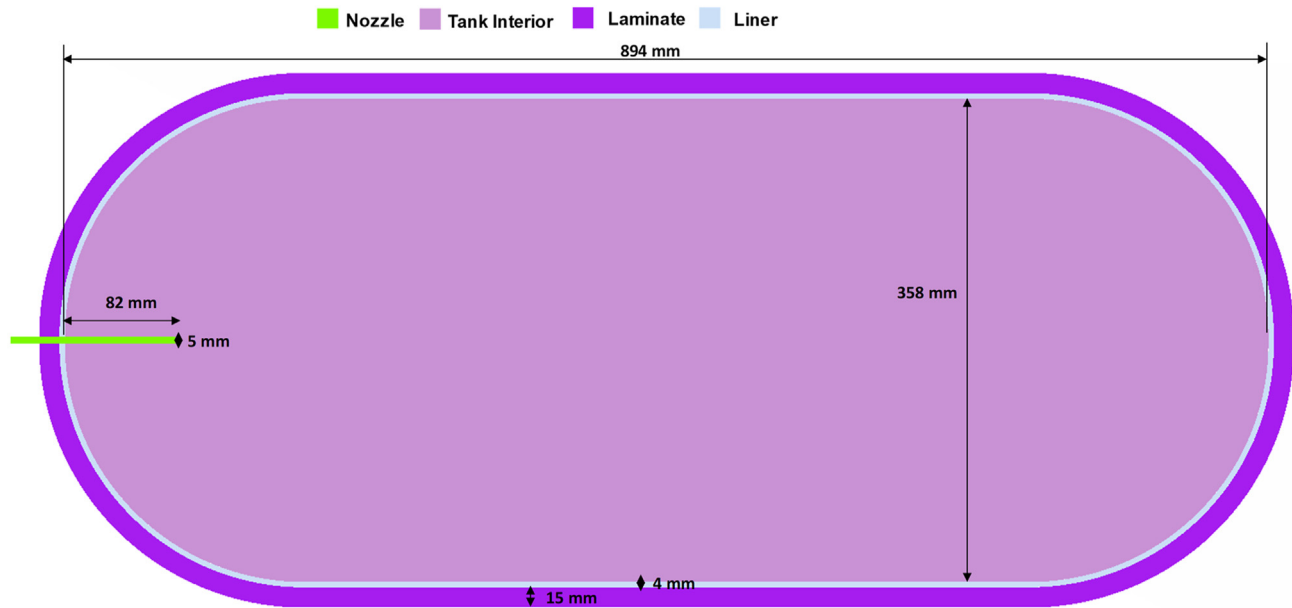


Fig. 1 – Geometry used for the 2D CFD analysis (Case 1: 2D CFD simulation of small H<sub>2</sub>-tank).

The SST  $k-\omega$  turbulence model was used for this study as it has the reputation of being robust and accurate enough to solve industry fluid dynamics problems. The SST  $k-\omega$  model incorporates an automatic selection mechanism for near wall turbulence modeling, which depends on the mesh resolution. When the value of  $y^+$  is less than one, the model uses the  $k-\omega$  model for near wall turbulence, whereas for  $y^+$  values greater than one, a wall function-based approach is employed. The wall  $y^+$  was about 500 in regions where the fluid jet effects were felt on the wall and around 5 in regions where they were not felt. The  $k-\epsilon$  model was utilized in regions located further away from the boundary layer.

The compressible real gas behavior was modeled using the Peng-Robinson equation of state. The equation of state, Poisson equation of pressure, momentum, and energy equations were discretized using a second-order scheme, while the turbulence conservation equations were discretized using a

first-order scheme. The pressure-velocity coupling was performed using the coupled algorithm. The pressure and temperature boundary conditions were implemented at the inlet. Nozzle inlet pressure and temperature measurements were made by Dicken and Mérida [13]. The data from these experiments were used to make polynomial curve fits for the pressure and temperature developments at the nozzle inlet (Fig. 3). These polynomial functions were then used to model the inlet pressure and temperature at the inlet boundary as a function of time, which made the simulated boundary conditions similar to the experiment.

The simulation time step was initially set to a very low value of 1E-6 s while carefully monitoring the critical parameters such as the CFL number, fluid velocity, pressure, and temperature. The residuals of mass, momentum, and energy equations were also closely monitored to ensure that the calculations converged. As the simulation progressed the time step was gradually increased to 1E-4 s to ensure a CFL number of 1. It should be noted here that in the 2D CFD modeling of the large H<sub>2</sub>-tank (Section 2.1.2) a time step of 1E-4 s was kept for the first 10 min of the simulation, after which it was adjusted to 5E-4 s and 1E-3 s to speed up the simulation while maintaining the CFL criteria. It is also worth noting here that as the filling time increased, the maximum fluid velocity inside the domain decreased, making it possible to increase the time step and speed up the simulations.

*Case 2: 2D CFD simulation of large H<sub>2</sub>-tank (Maritime case)*  
Data from a commercial provider of pressurized hydrogen tanks was used as a basis for the 2D CFD simulations made in Case 2 (large H<sub>2</sub>-tank for the maritime). The large H<sub>2</sub>-tank analyzed has a length of 5.77 m and a diameter of 650 mm which gives an internal volume of about 2000 L (i.e., more than 25 times larger than the small H<sub>2</sub>-tank in Case 1). The H<sub>2</sub>-tank analyzed was assumed to have two layers of insulation, a liner with a thickness of 3 mm, and a glass fiber layer with a

Table 1 – Summary of simulation parameters in the 2D CFD simulation of the small H<sub>2</sub>-tank (Case 1).

Parameter	Value
Software	Ansys Fluent, 2020 R1
Mesh type	Quadrilateral (majority cells) and Triangular
Model	2D, Axisymmetric
Solver type	Pressure-based (coupled scheme), implicit solver
Simulation type	Transient
Turbulence model	SST $k-\omega$
Fluid	Hydrogen (default Fluent material properties). Fluid density is modeled using Peng-Robinson equation of state model.
Time step	Variable (criteria is to have Courant number <1)



Fig. 2 – Computational mesh for the 2D CFD analysis (Case 1: 2D CFD simulation of small H2-tank).

thickness of 63 mm. The insulation material properties assumed are described in Table 2. The H<sub>2</sub> inlet flow was assumed to enter the tank via a single nozzle with a 4 mm diameter.

The CFD-simulations performed in Case 2 was assumed to be axisymmetric (as in Case 1). It should be noted here that the ends of the H<sub>2</sub>-tank are spherical shapes (with curved ends in 2D). The curved ends of the H<sub>2</sub>-tank are modeled in the 2D CFD simulations but are not shown in full detail in the simplified 2D (square) figures below. The geometry of the calculation domain used in the 2D CFD-simulations of the large H<sub>2</sub>-tank is shown in Fig. 4. A simplified schematics showing the main calculation domain analyzed and the mesh used for the 2D CFD simulation is shown in Fig. 5. Only quadrilateral elements are used, with the minimum and maximum cell sizes of 1 mm and 20 mm, respectively. The smaller elements are placed in the region where velocity gradients are expected to be the largest. The size of the cells in these simulations were fixed at 1 mm near the walls and in regions where large velocity gradients were expected. The total number of computational cells used in the 2D CFD simulations of the large H<sub>2</sub>-tank was approximately 11,000, with a wall  $y^+$  of around 300 in regions where fluid jet effects were

felt on the wall and a wall  $y^+$  of around 5 where fluid jet effects were not felt on the wall.

A fast-filling scenario was assumed in the 2D CFD simulation of the large H<sub>2</sub>-tank. The tank pressure was in this scenario increased linearly from 20 bar (initial pressure) to 350 bar over 20 min (ca. 1 kg H<sub>2</sub> per minute), while the inlet temperature of the hydrogen gas was kept at a constant value of 20 °C. The ambient temperature was set to 27 °C (300 K) and a heat transfer coefficient of  $6 \text{ W m}^{-2} \text{ K}^{-1}$  was assumed (both in Case 1 and Case 2), to ensure that the heat transfer rate from the system to the surroundings remained low. The CFD methodology applied in the 2D CFD simulations of the large H<sub>2</sub>-tank was similar to that of the smaller H<sub>2</sub>-tank (Section 0).

#### One-dimensional model for wall heat transfer

A model for studying the heat transfer in the tank wall was developed for this study. This model was based on a one-dimensional (1D) discretization of the wall (cylindrical coordinates) and a zero-dimensional (0D) model for the hydrogen. The non-dimensional model was presented by Molkov et al. [10] and has been validated for smaller tank volumes for hydrogen up to 700 bar and is shown in Equation (1):

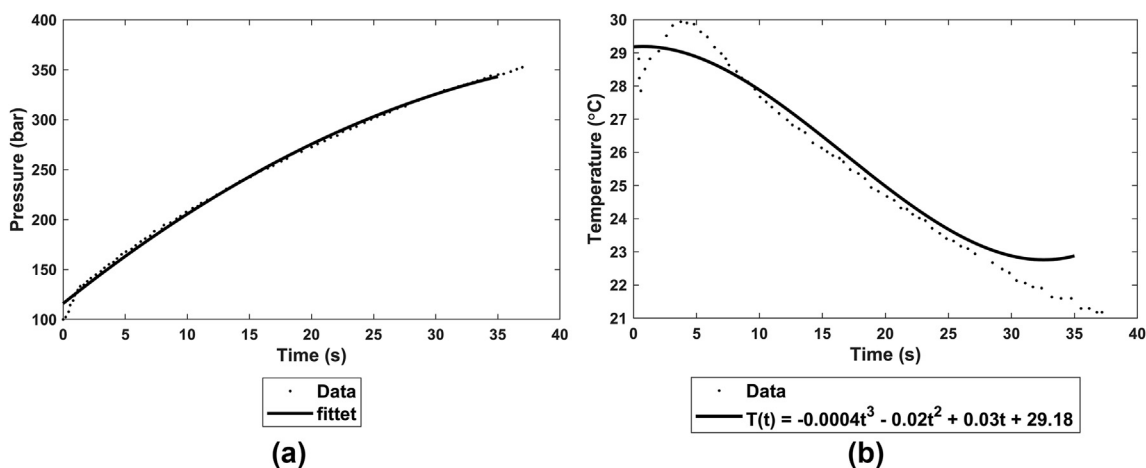


Fig. 3 – Nozzle inlet pressure and temperature as a function of time (boundary conditions). Polynomial functions (based on experimental data) used in 2D CFD simulation of the small H<sub>2</sub>-tank (Case 1).



**Table 2 – Properties for the insulation materials use in the simulations of the large H2-tank (Case 2).**

Property	Value	Unit
Liner density	945	(kg·m <sup>-3</sup> )
Liner specific heat	1580	(J·kg <sup>-1</sup> K <sup>-1</sup> )
Liner thermal conductivity	0.48	(W·m <sup>-1</sup> K <sup>-1</sup> )
Glass-Fiber density	2051	(kg·m <sup>-3</sup> )
Glass-Fiber specific heat	878	(J·kg <sup>-1</sup> K <sup>-1</sup> )
Glass-Fiber thermal conductivity	0.113	(W·m <sup>-1</sup> K <sup>-1</sup> )

$$\frac{dm_t}{dt} = \frac{\frac{1}{\gamma-1} \left( (V_t - b m_t) \frac{dp_t}{dt} \right) - \frac{dQ}{dt}}{\frac{1}{\gamma-1} (bp_t) + C_{p,e} T_e} \quad (1)$$

where pressure ramp function  $\frac{dp_t}{dt}$  is an input parameter to the model.

The convection heat transfer rate from hydrogen to the inner wall of the tank  $\frac{dQ}{dt}$  is given by Equation (2):

$$\frac{dQ}{dt} = A_{s_i} h_g (T_{s_i} - T_t) \quad (2)$$

The model for convective heat transfer coefficient  $\frac{dQ}{dt}$  accounts for the natural and forced convection between the gas and the inner tank wall (A more detailed description of this model can be found in Ref. [10]). The heat transfer through the tank wall is discretized to include the temperature gradient through the wall during filling and to account for several different layers of materials such as liner and fiber-reinforced polymer. The tank wall heat flow is modeled as a pipe wall heat flow, neglecting the hemispherical shape effects of the end sections of the tanks. The transient heat transfer equations solved in cylindrical coordinates can be expressed by Equation (3):

$$\frac{\partial T}{\partial t} = \frac{1}{C_{p,wall} m_{wall}} \frac{1}{r} \frac{\partial}{\partial r} \left( kr \frac{\partial T}{\partial r} \right) \quad (3)$$

In Equation (3), the time derivative is discretized with the forward Euler method, and the spatial derivative is discretized with the second-order central-difference scheme. Fig. 6 illustrates the discretization of the walls (cylindrical) used in the 1D modeling, including the inner and outer walls, details on the calculation domains, surface and ambient temperatures, and volume interface radiuses. MATLAB was used for the 1D modeling.

### Zero-dimensional model

A simplified zero-dimensional (0D) model was also developed in this study. The 0D model was implemented in the Engineering Equation Solver (EES) program to make it possible to perform quicker calculations and rapid screening of the average temperature development during the tank filling. The EES model solves a set of equations that describe the system and a set of non-linear and differential equations that represent the mass and energy balance for the bunkering process.

In the 0D model the following two main simplifications were made: (1) No fluid dynamics effects were included and (2) The heat transfer to the wall was based on an average heat capacity for the entire tank wall. In the 0D model in EES a simplified approach for estimating the heat transfer from the gas to the tank wall is assumed. Hence, the 0D model did not include discretization of the tank wall nor any calculations of the heat transfer from gas to inner wall surface, through wall, and from the outer wall surface to the surroundings, as was the case in the 1D model (Section 2.2). Instead, there was made a crude assumption that the part of the wall with heat capacity has the same temperature as the hydrogen gas and that the rest of the wall material is unaffected. In other words, in the 0D model the mass of the wall material was assumed to work as a heat sink, resulting in a gas temperature that is lower compared to pure adiabatic conditions. The real gas model by Leachman et al. [13] (included in EES) was used for the thermodynamic state calculations. The model describes the filling of a hydrogen tank from a constant source at a pressure of 45 MPa and a temperature of 293.15 K.

The mass and energy balance for the tank-filling process can be expressed by the following equations:

$$\frac{dU_t}{dt} = \dot{m}_e \cdot h_e \quad (4)$$

where the total internal energy in the tank at time = 0 can be calculated by:

$$U_{\text{tank},t=0} = m_{H_2,t=0} \cdot u_{t=0} + C_{\text{wall}} \cdot T_{\text{amb},t=0} \quad (5)$$

and the internal energy in the tank at time = 2 can be calculated by:

$$U_2 = m_2 \cdot u_2 + C_{\text{wall}} \cdot T_2 \quad (6)$$

In the equations  $U_t$  denotes the internal energy of the gas inside the tank,  $m_e$  the mass of hydrogen in the tank, and  $h_e$

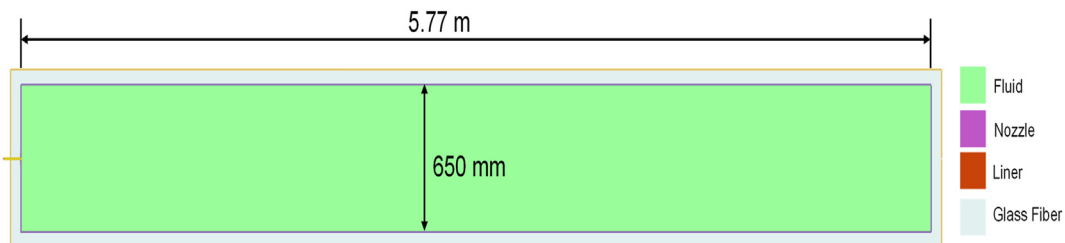


**Fig. 4 – Geometry and dimensions (Case 2: Large H2-tank for maritime).**

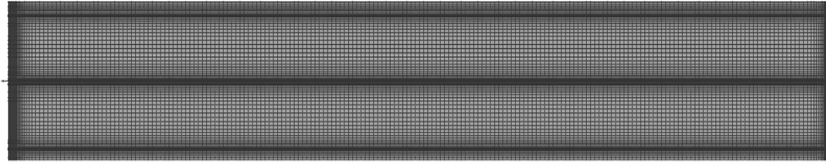


Fig. 5 – Computational mesh (Case 2: Large H2-tank for maritime).

denotes the enthalpy of the hydrogen inlet flow. It should also be noted that in Equation (6) the total heat capacity of the wall  $C_{\text{wall}}$  is assumed to have the same temperature as the hydrogen gas. The value of  $C_{\text{wall}}$  (kJ/K) is calculated by multiplying the mass of the wall material with the specific heat capacity of the wall material.

A graphical user interface (GUI), or a so called *EES Diagram Window*, was developed for the EES model (Fig. 7). In the GUI it is possible for the user to choose either a constant mass flow rate or a mass flow rate that decreases as a function of time. The EES model is available as a distributable program that can be downloaded for free by contacting the authors.

## Results and discussion

The main objective with this part of the study was to analyze and compare the performance of the three different models developed. Since the overall goal in the main project was to integrate a simplified hydrogen tank model into a larger hydrogen refueling system model in EES, it was particularly

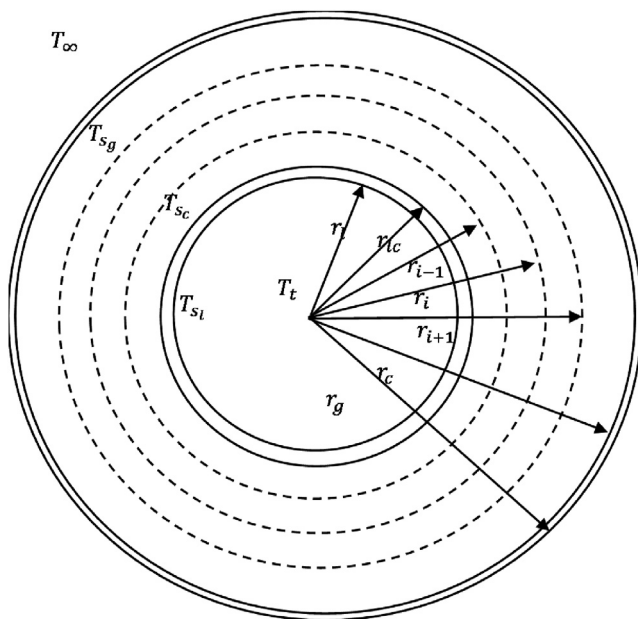


Fig. 6 – Illustration of 1D wall discretization in a cylindrical tank, including the inner and outer walls, details on the calculation domains  $[r_{i-1}, r_i]$ , surface and ambient temperatures, and volume interface radiuses.

important to investigate how the 0D model (Section 2.3) compared to the more detailed 1D model (Section 2.2) and the 2D CFD-model (Section 2.1).

### Results from modeling of small H2-tank (Case 1)

The mean fluid temperature inside the H2-tank is the key variable to be validated. A comparison between the three models developed and the measurements derived from Dicken and Mérida [13] is shown in Fig. 8. The results show that there is an excellent agreement between the 2D CFD-predictions and the measurements, which gives confidence to apply the CFD-method to larger H2-tanks (e.g., H2-tanks for maritime applications). The measurements were also compared to the calculations made using the simpler 1D model in MATLAB and the even more simplified 0D-model in EES. The predictions from the two simpler models are reasonable, both showing trends that are consistent with the experimental results. The small difference between the measurements and the predictions are likely to come from the limited number of thermocouples installed inside the small-scale experimental H2-tank. Dicken and Mérida [13] made measurements at 63 locations inside the H2-tank, but this does not cover the entire volume of the tank. In comparison, the CFD-model accounts for the entire volume of the H2-tank and assumes that there is an axisymmetric boundary condition. The results from the 1D-model match well with the experimental result for smaller H2-tanks, but the best results are provided by the 2D CFD-model.

A 2D axisymmetric CFD-simulation of 35 s takes approximately 8 days of CPU time on an 8-core Intel®Xeon®W-2145 processor (3.7 GHz) with 64 GB of RAM, while the simulation of the 1D-model in MATLAB only takes a few minutes. When the correct input data is supplied to the 1D-model it can be executed very quickly. The 0D-model in EES takes a while to set up the first time, since user-defined equations must be established and integrated with the built-in functions in the program. However, once this has been done the actual simulation time is relatively short. Hence, both the 1D-model in MATLAB and the 0D-model in EES are more suitable for more general studies on hydrogen refueling, while the 2D CFD-model in Ansys-Fluent is more suitable for detailed studies on flow and thermal behavior inside the H2-tank.

Fig. 9 shows the velocity and temperature contours inside the tank for several time steps. The hydrogen gas is in this case entering the tank through a nozzle as a high-speed jet, which can result in better gas mixing inside the tank. The maximum velocity of the jet decreases with an increase in

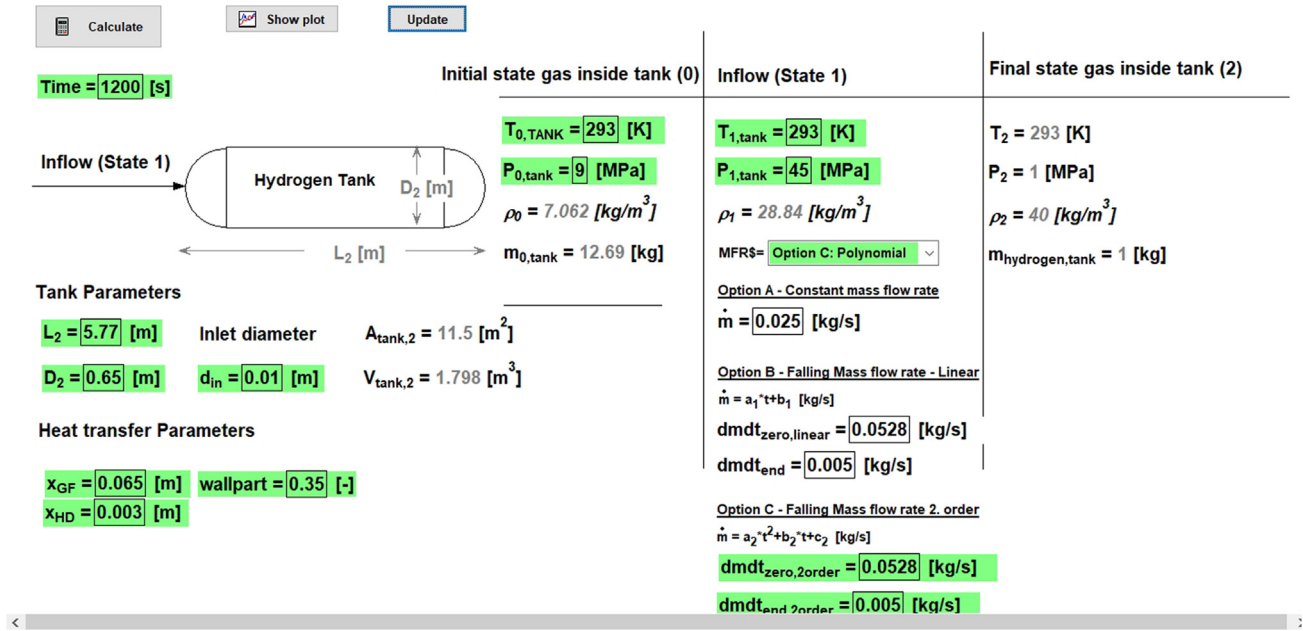


Fig. 7 – The graphical user interface (GUI) for the H2-tank 0D model in EES. Note that the green boxes contain input parameters that can be easily entered by the user. (For interpretation of the references to color in this figure legend, the reader is referred to the Web version of this article.)

filling time. This can be better explained by calculating the Reynolds number based on hydrogen gas and flow properties obtained at the nozzle inlet (density, viscosity, velocity, and nozzle diameter). Fig. 10 shows that the Reynolds number decreases with an increase in time. (Due to increase in pressure inside the tank over time which leads to a gradual increase in fluid density).

In Fig. 9 it can also be observed how the hydrogen flow jet propagates into the center of the tank. This has an important

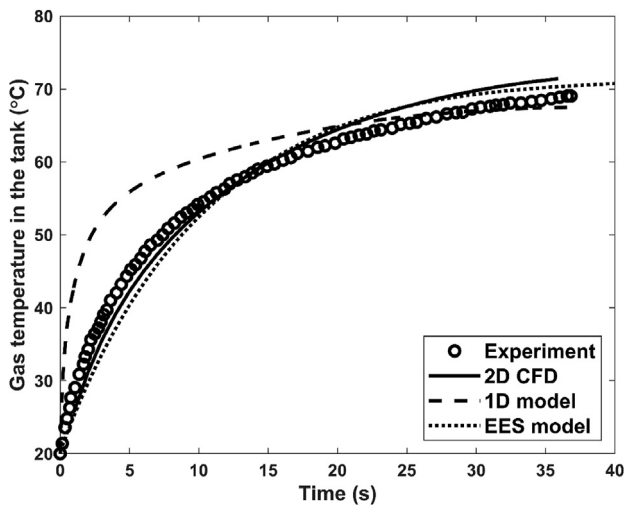


Fig. 8 – Gas temperature development inside the small H2-tank. Comparison of developed models (2D CFD, 1D, and 0D) against measurements made by Dicken and Mérida [13].

effect on the temperature distribution inside the tank; the temperature contour plots show a nearly uniform temperature distribution within the tank, except near the jet region. (The temperature of the fluid inside the jet depends on fluid expansion behavior, which in turn is dependent on pressure ratio). From this it can be concluded that for filling of small H2-tanks the temperature distribution inside the tank will be uniform due to the effect of the jet (resulting in better flow mixing) throughout the entire tank volume. It can also be observed that the fluid temperature inside the small H2-tank does not differ significantly from the rest of the tank in any specific area.

The temperature distribution inside the H2-tank is related to the convection heat transfer. Results from the 2D CFD calculations were therefore used to estimate the internal heat transfer coefficient (*IHTC*). The internal heat transfer coefficient was derived from the following expression:

$$h_g = \frac{\dot{Q}}{A_{s_i} (\bar{T}_t - \bar{T}_{s_i})} \tag{5}$$

where  $\dot{Q}$  is the heat transfer rate,  $\bar{T}_t$  is the mean fluid temperature inside the tank,  $\bar{T}_{s_i}$  is the mean temperature of the wall surface in contact with the fluid, and the parameter  $A_{s_i}$  is the surface area of for the heat transfer. Fig. 11 shows the internal heat transfer coefficient *a* as a function of time (time for a H2-filling), with minimum and maximum values for *IHTC* at  $402 \text{ W}\cdot\text{m}^{-2}\text{K}^{-1}$  and  $1750 \text{ W}\cdot\text{m}^{-2}\text{K}^{-1}$ , respectively. The results show how the internal heat transfer coefficient decreases over the time of the H2-filling. This is because the mean fluid velocity inside the tank decreases with time, resulting in less heat transfer.

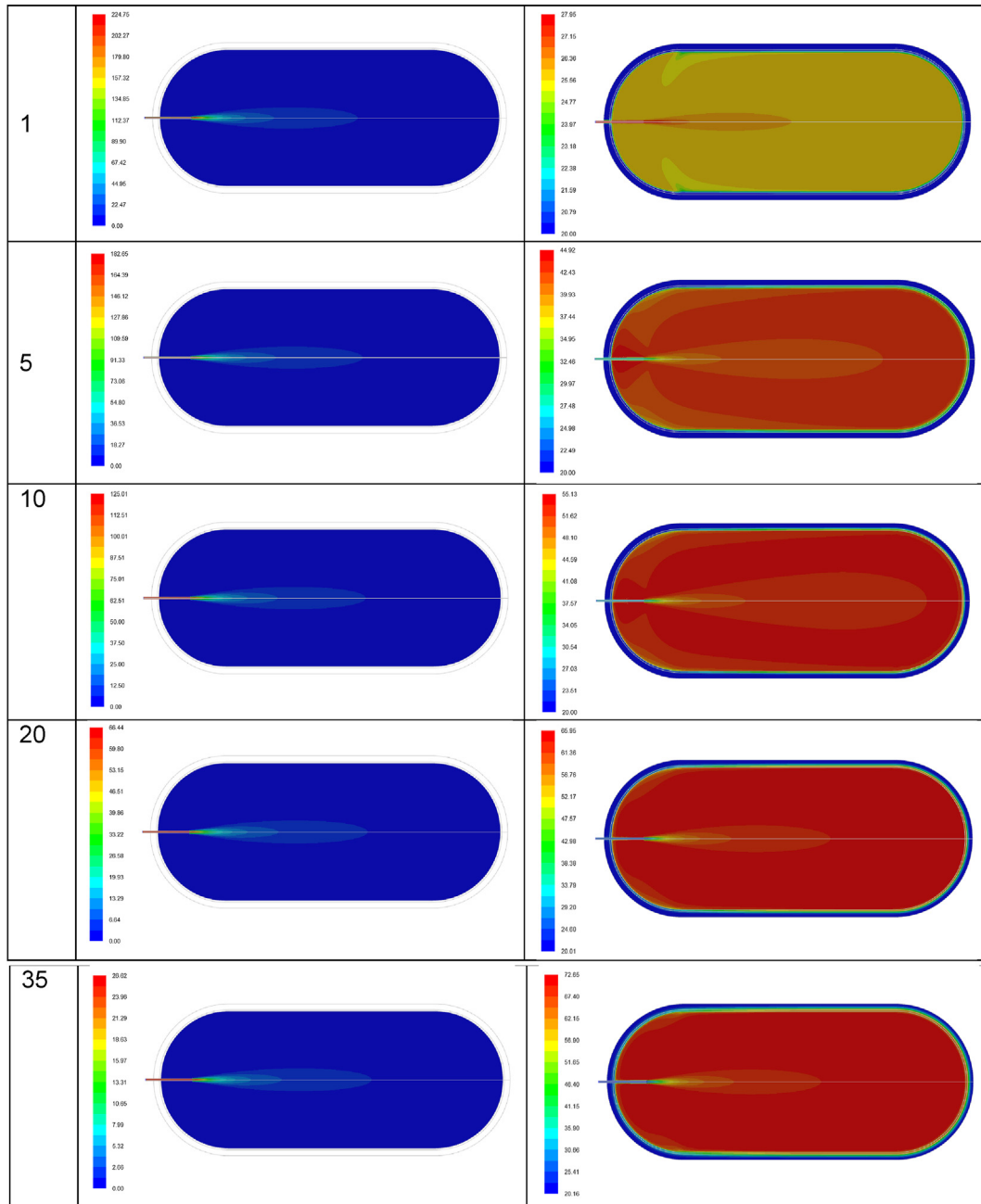


**Fig. 9** – Results from the 2D CFD simulations of fluid velocity ( $\text{m}\cdot\text{s}^{-1}$ ) contours (plots on the left) and temperature ( $^{\circ}\text{C}$ ) contours (plots on the right) at different times during the fast-filling of a small H<sub>2</sub>-tank.

### Results from modeling of large H<sub>2</sub>-tank (Case 2)

The CFD results for the simulation performed on a large H<sub>2</sub>-tank geometry are presented in this section. The CFD-model and methodology validated for the small H<sub>2</sub>-tank was applied to a larger H<sub>2</sub>-tank. A fast-filling scenario with a H<sub>2</sub>-filling time of 20 min was assumed in the CFD-simulations. It took about 24 days of CPU time to perform the CFD-simulation on an 8-core Intel®Xeon®W-2145 processor

(3.7 GHz) with 64 GB of RAM. Details on the settings for the CFD-simulation are found in Section 2.1.2.

Fig. 12 shows the mean temperature of the fluid inside the tank with time and the mean temperature of the wall surface in contact with the fluid. The simulations in the 1D-model, which uses a zero-dimensional volume solver for the hydrogen, were based on a convective heat transfer coefficient derived from the 2D CFD-simulation and simplified to be a constant  $40 \text{ W}\cdot\text{m}^{-2}\text{K}^{-1}$ . The 2D CFD-simulation



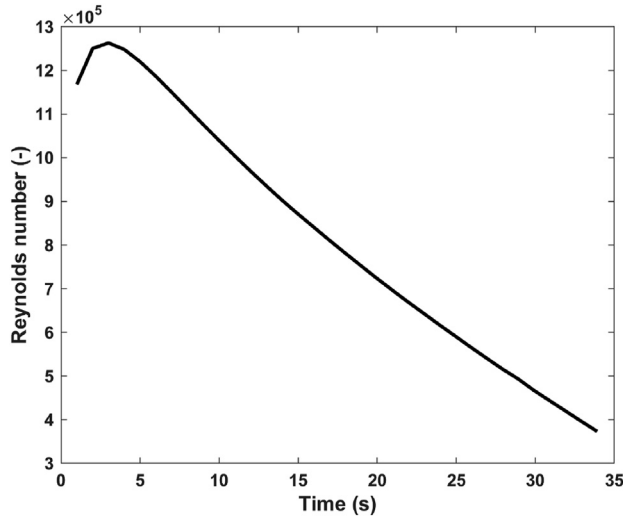


**Fig. 10** – Reynolds number calculated based on inlet fluid properties at the nozzle inlet.

estimated that for a H<sub>2</sub>-tank filling time of 20 min the mean fluid temperature of the fluid would reach a value above 100 °C. This temperature is beyond the acceptable maximum temperature of the liner material. Hence, the average temperature of the liner material surface was carefully monitored during the simulation and set to a maximum of 90 °C. Section 2.2 describes the simple modifications made to the original heat transfer coefficient model. Further research is needed to develop a more explicit heat transfer coefficient model that takes tank size and filling time into consideration.

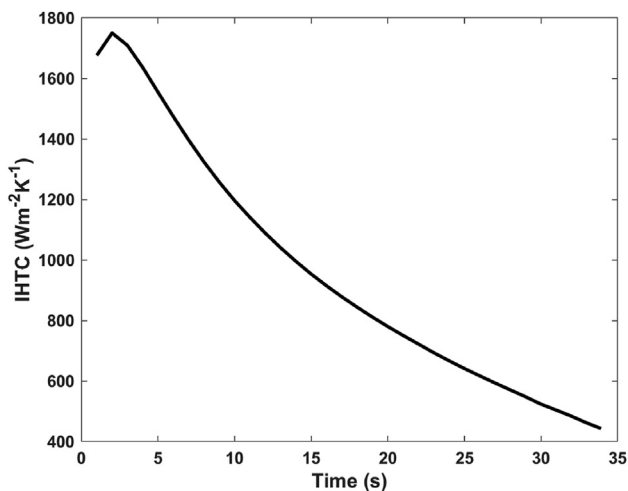


**Fig. 11** – Internal Heat Transfer Coefficient (IHTC) calculated using the mean temperature of the fluid, average surface temperature of the wall, heat transfer rate, and the surface area.

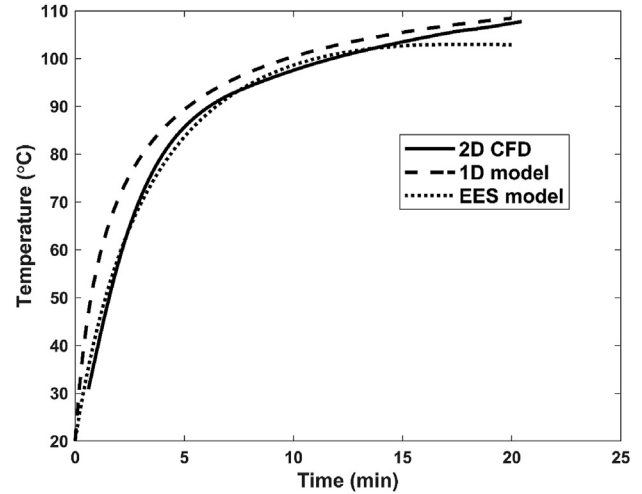


**Fig. 12** – Mean temperature development as a function of time for filling the maritime-sized hydrogen tank.

**Fig. 13** show the temperature distribution inside the large H<sub>2</sub>-tank at different instantaneous times (1, 3, 4, and 20 min) during the filling. According to the contour plots, the temperature distribution of the fluid inside the larger H<sub>2</sub>-tanks is not homogeneous, as opposed to the homogeneous behavior found in the smaller H<sub>2</sub>-tanks. The temperature of the fluid at the far end of the H<sub>2</sub>-tank is much higher than elsewhere. It should be noted here that the 2D models do not consider natural convection effects, which can have a significant impact on fluid flow and thermal distribution in the azimuthal direction. Three-dimensional simulations are required to fully capture these effects. However, since natural convection effects are more pronounced for slow filling it can be justified to use 2D models for simulation of fast filling of hydrogen. In any case, the heating taking place at the end of long H<sub>2</sub>-tanks during fast-filling should be confirmed in future 3D CFD simulations that also include natural convection effects.

It is possible to explain the inhomogeneous temperature distribution inside the H<sub>2</sub>-tank by looking at the velocity contours shown in **Fig. 14**, e.g., the velocity contour at the 20-min simulation time instance. Here it can be noticed that the high velocity jet effect is not influencing the behavior of the gas at the far end of the large and long H<sub>2</sub>-tank. It can be observed that the gas is moving at a velocity of about 0.01 m s<sup>-1</sup> at the far end of the tank. It is also possible to observe the mixing region to explain the temperature distribution in the tank. This can be achieved by plotting the stream function, as shown at the 20-min time instance in **Fig. 15**. The region adjacent to the nozzle where fluid mixing occurs is shown in the plot. This contour plot indicates that fluid mixing occurs for approximately 28% of the tank length. In other words, the mixing of the gas is weaker further out in the longitudinal direction of the H<sub>2</sub>-tank. This will affect heat transfer from the H<sub>2</sub>-tank to the surroundings. A similar temperature profile has been observed by Carrere et al. [14].

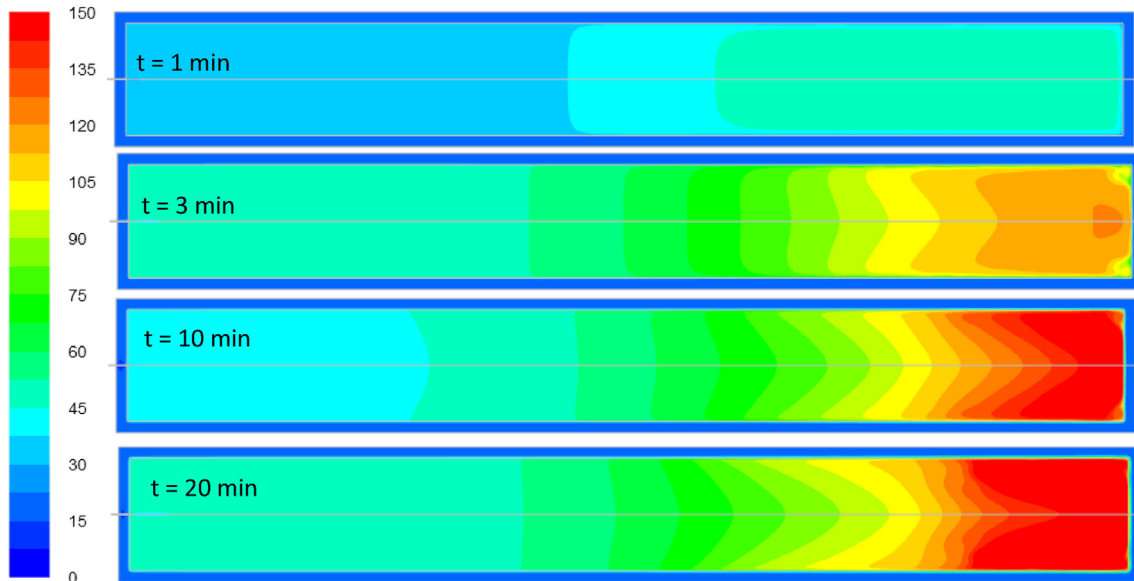


Fig. 13 – Result from 2D CFD simulation of a large H<sub>2</sub> tank. Temperature (°C) distribution inside the tank at four different time intervals: 1, 3, 10, and 20 min.

It may be possible to enhance heat transfer if there is sufficient mixing at the far end of the tank. Here it should be noted that the outer material assumed in this study (glass fiber) has a greater capacity to absorb heat. Fig. 16 shows the internal heat transfer coefficient calculated from the simulations of the large H<sub>2</sub>-tank, where the maximum and minimum heat transfer coefficient values were calculated to be  $90 \text{ W}\cdot\text{m}^{-2}\text{K}^{-1}$  and  $36 \text{ W}\cdot\text{m}^{-2}\text{K}^{-1}$ , respectively. The heat transfer coefficient value for the small H<sub>2</sub>-tank is very low

compared to the large H<sub>2</sub>-tank. This result also explains the presence of high temperature zones inside the large H<sub>2</sub>-tank.

The results in this study confirm the need to pre-cool the hydrogen during the fast filling of H<sub>2</sub>-tanks, which is common practice in hydrogen refueling stations for road transport. It can also be confirmed that for large H<sub>2</sub>-tanks the convection heat transfer coefficient must be modeled based on fluid dynamics phenomena. The results from the 2D CFD simulations show how the internal flow in large H<sub>2</sub>-tanks will only mix the fluid



Fig. 14 – Result from 2D CFD simulation of a large H<sub>2</sub> tank. Velocity magnitude distribution inside the tank at 20 min time instance. Velocity values are shown in m/s.

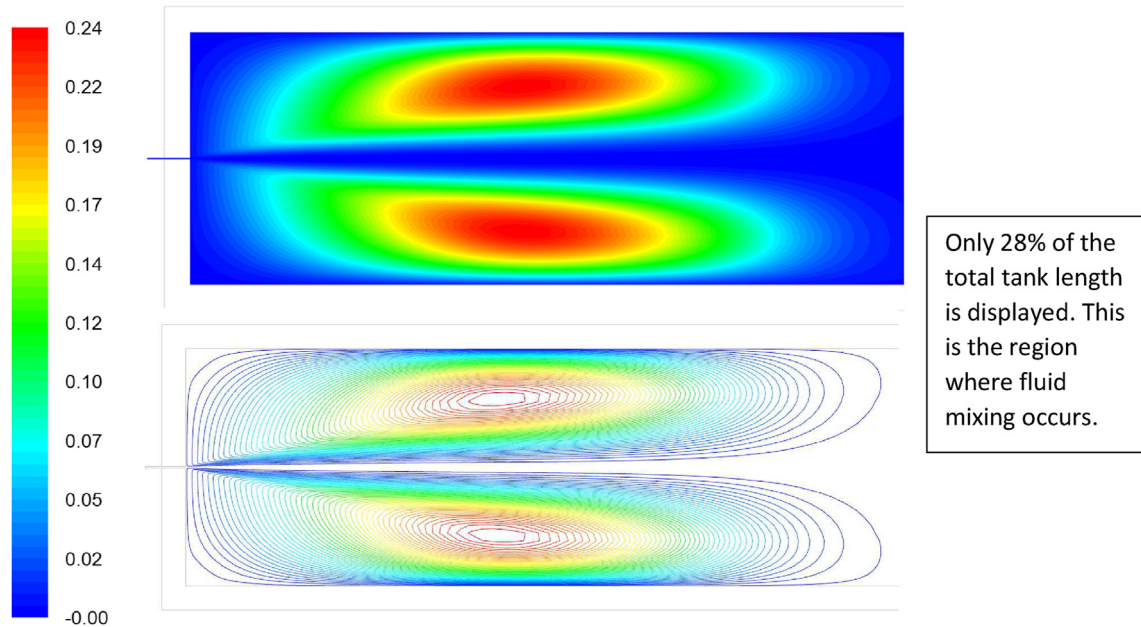


**Fig. 15** – Result from 2D CFD simulation of a large H<sub>2</sub> tank. Fluid mixing region at 20 min time instance illustrated using stream function ( $\text{kg}\cdot\text{s}^{-1}$ ) in Ansys-Fluent.

(H<sub>2</sub>) locally and herby influence the heat transfer. Finally, it should be noted that no buoyancy effects were included in the 2D CFD simulations. This might have a significant effect on both mixing and heat transfer, especially for slow filling processes.

#### Effect of heat transfer in the tank wall

The one-dimensional model was used to study the effect of heat transfer in the wall on the fluid temperature during filling. The convective heat transfer coefficient of of

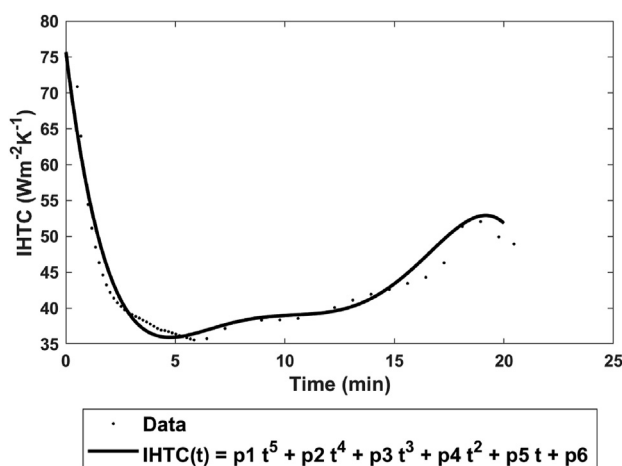


**Fig. 16** – Internal Heat Transfer Coefficient (IHTC) calculated for the large H<sub>2</sub>-tank simulation, where:  
 $p1 = -6.267e - 13$ ,  $p2 = 2.106e - 09$ ,  $p3 = -2.636e - 06$ ,  $p4 = 0.001537$ ,  $p5 = -0.4081$ ,  $p6 = 75.7$ .

$40 \text{ W}\cdot\text{m}^{-2}\text{K}^{-1}$  was taken from the CFD simulation, while the higher coefficients were included as a parameter study. Fig. 17 shows how convective the heat transfer coefficient values ( $40$ ,  $200$ , and  $1000 \text{ W}\cdot\text{m}^{-2}\text{K}^{-1}$ ) affects the heat transfer through the tank wall during filling of the large H<sub>2</sub>-tank and how these coefficients control the heat transfer between the hydrogen gas and the inner tank wall surface. The results from the 1D-model show that by increasing the convective heat transfer coefficient, the inner wall temperature increases. If the temperature difference between the hydrogen gas and the wall decreases (middle figure), the heat transfer will be reduced. Another observation that can be made is that there is no significant heating of the wall, i.e., the heat capacity of the H<sub>2</sub>-tank itself cannot be utilized for effectively cooling of the hydrogen. The low thermal conductivity of the tank wall material and the relatively lower heat transfer area compared to the tank volume will hinder effective heat transfer and cooling of the hydrogen during filling (bottom figure).

Finally, when comparing the results from the simulations and modeling of the small and large H<sub>2</sub> tanks it is also important to have in mind the slight physical difference in materials used in the tanks. The small H<sub>2</sub>-tank studied (with data from Ref. [13]) was a Type III tank with aluminum liner with a high thermal conductivity and heat capacity, while the large H<sub>2</sub>-tank had a polymer liner. A closer look at the wall temperature profile shows that the internal energy is accumulated in regions close to the liner and fluid. In a H<sub>2</sub>-tank with an inner aluminum liner this heating effect will be smaller since it will contribute to the cooling of the hydrogen gas by keeping the inner wall temperature lower compared to a tank with a polymer liner.

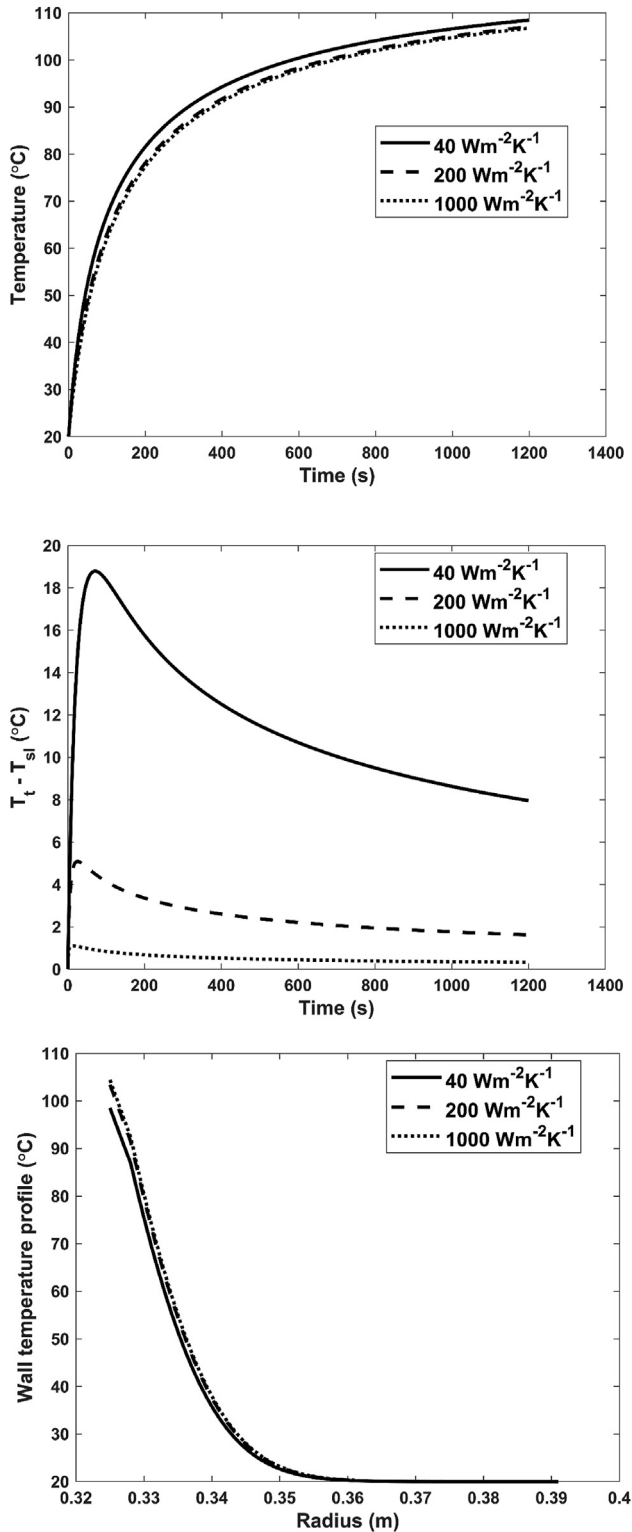


**Fig. 17 – Results from 1D modeling of a large H<sub>2</sub>-tank using different convection heat transfer coefficients** Top figure: Mean hydrogen temperature in the tank during filling, Middle figure: Temperature difference between hydrogen gas and inner tank wall. Bottom figure: Temperature profile through the wall at 20 min.

## Conclusions & recommendations

The main objective with this study has been to establish a set of numerical simulations tools suitable for modeling of the fast fueling of compressed gaseous hydrogen, with focus on estimating the temperature development inside large hydrogen tanks suitable for maritime applications. Three numerical models with different dimensions and complexity have been developed, validated, and compared: (1) 2D CFD model in Ansys-Fluent (2) 1D-model in MATLAB, and (3) 0D-model in EES.

The results show that 2D CFD simulations can be used to calculate the flow and thermal field inside a H<sub>2</sub>-tank. Based on the two detailed CFD simulations performed in this study, one for a small H<sub>2</sub>-tank (Case 1) and one for a large H<sub>2</sub>-tank (Case 2), it can be concluded that the effective fluid mixing caused by the turbulent jet flow will enhance heat transfer and achieve a nearly uniform temperature distribution in the entire volume in a small H<sub>2</sub>-tank. However, this is not the case with fast filling of gaseous hydrogen in a larger H<sub>2</sub>-tank.

For the large H<sub>2</sub>-tank the CFD results suggest that fluid mixing is only confined to 28% of the tank length (measured from the nozzle inlet). The temperature distribution of the fluid inside the tank was not homogeneous in this case, as opposed to the homogeneous behavior found in the smaller H<sub>2</sub>-tank. In the large H<sub>2</sub>-tank the temperature of the fluid at the far end of the tank was found to be much higher than elsewhere. Hence, the CFD simulations performed in this study indicate that it will be important to monitor temperature in the during fast filling of hydrogen. In actual systems, a temperature sensor should be placed at the end of the tank to monitor the temperature where the heat transfer rate is likely to be low.

The 2D CFD models in this study do not consider buoyancy or natural convection effects, which can have a significant impact on fluid flow and thermal behavior in the tank. Three-dimensional CFD simulations would be required to fully capture these effects. The heating taking place at the end of large and long H<sub>2</sub>-tanks during fast-filling should be confirmed in future 3D CFD simulations that also include natural convection effects. However, since natural convection effects are more pronounced for slow filling it can probably be justified to use 2D CFD models for simulation of fast filling of hydrogen.

It was also demonstrated in this study that the 0D and 1D-models developed can predict the overall temperature and pressure development during the fast-filling of H<sub>2</sub>-tanks. The 1D wall discretization model can capture important effects that control the main cooling of hydrogen during filling. However, the 1D model will not be able to capture the local high temperature regions (hot spots) since it assumes a mean (bulk) temperature for hydrogen in the tank. A detailed analysis of the fast-filling of a large H<sub>2</sub>-tank showed how the internal heat transfer coefficient in the tank can limit the cooling of the gas.

Finally, a recommendation for future work is to set up an experimental campaign to study flow and thermal fields



during a fast-filling process of a large H<sub>2</sub>-tank. The experimental data could then be used to validate 2D and 3D CFD models and to develop a better internal heat transfer coefficient model that can be incorporated into the 1D-model. The results from such experiments and model validations would be very useful when generating recommendations and practices on how to perform safe and energy efficient fast filling of large H<sub>2</sub>-tanks suitable for maritime applications.

### Declaration of competing interest

The authors declare that they have no known competing financial interests or personal relationships that could have appeared to influence the work reported in this paper.

### Acknowledgments

The work presented in this paper was part of the H2Maritime-project (*Hydrogen and Fuel Cell for Maritime Applications*) and funded by the Research Council of Norway (RCN project no. 294568) and five industry partners.

### Abbreviations

Ansys-Fluent	Fluid simulation software
CFD	Computational Fluid Dynamics
CFL	Courant–Friedrichs–Lewy
CPU	Central processing unit
EES	Engineering Equation Solver program
GUI	Graphical User Interface
H <sub>2</sub>	Hydrogen
IHTC	Internal Heat Transfer Coefficient
MATLAB	Multi-paradigm programming language
RAM	Random-Access Memory
SST	Shear Stress Transport
0D, 1D, 2D, 3D	Zero-Dimensional, One-Dimensional, Two-Dimensional, Three-Dimensional

### Nomenclature

A	Surface area, (m <sup>2</sup> )
b	Correction coefficient of specific volume in the Abel-Noble equation, $7.691 \times 10^{-3}$ (m <sup>3</sup> kg <sup>-1</sup> ) [15,16]
$c_{p_{wc}}$	Specific heat capacity of composite material, (J·kg <sup>-1</sup> K <sup>-1</sup> )
$c_{p_{wl}}$	Specific heat capacity of liner material, (J·kg <sup>-1</sup> K <sup>-1</sup> )
$c_{p_e}$	Specific heat capacity of gas at the inlet, (J·kg <sup>-1</sup> K <sup>-1</sup> )
$c_{v,t}$	Specific heat capacity of gas at the tank, (J·kg <sup>-1</sup> K <sup>-1</sup> )
$d_e$	Nozzle diameter, (m)
$h_g$	Convective heat transfer coefficient of hydrogen, (W·m <sup>-2</sup> K <sup>-1</sup> )
$H_e$	Enthalpy of inlet flow, (J·Kg <sup>-1</sup> )
$m_e$	Tank inlet mass, (kg)
$\dot{m}_e$	Tank inlet mass flow rate, (kg·s <sup>-1</sup> )
$\dot{n}_e$	Tank inlet molar flow rate, (kmols <sup>-1</sup> )
$k_{wl}$	Conduction coefficient of liner wall, (W·m <sup>-1</sup> K <sup>-1</sup> )
$k_{wc}$	Conduction coefficient of composite wall, (W·m <sup>-1</sup> K <sup>-1</sup> )
$p_t$	Tank pressure, (MPa)

$p_{t_0}$	Initial tank pressure, (MPa)
$p_{t_0}$	Final tank pressure while filling, (MPa)
Q	Heat transfer, (J)
r	Tank radius, (m)
$R_{H_2}$	Gas constant, 4124.2 (J·kg <sup>-1</sup> K <sup>-1</sup> )
$\Delta t$	Time step, (s)
$T_e$	Inlet gas temperature, (K)
$T_t$	Tank gas temperature, (K)
U	Internal energy, (J)
$\beta$	Coefficient of thermal expansion, (K <sup>-1</sup> )
$\gamma$	Specific heat ratio
$\rho_e$	Density of inlet hydrogen, (kg·m <sup>-3</sup> )
$\rho_{wc}$	Density of composite material, (kg·m <sup>-3</sup> )
$\rho_{wl}$	Density of liner material, (kg·m <sup>-3</sup> )
Subscript c	Carbon fiber/epoxy composite wall, the middle layer
Subscript e	Inlet or inject
Subscript g	Glass fiber/epoxy composite wall, the outer layer
Subscript l	Liner wall
Subscript s	Surface
Subscript t	Inside the tank
Subscript w	Wall
Subscript $\infty$	Tank outside atmosphere
Subscript 0	Initial condition

### REFERENCES

- [1] Galassi MC, Papanikolaou E, Heitsch M, Baraldi D, Iborra BA, Moretto P. Assessment of CFD models for hydrogen fast filling simulations. *Int J Hydr Energy* 2014;vol. 39:6252–60. <https://doi.org/10.1016/j.ijhydene.2013.03.164>. Elsevier Ltd.
- [2] Liu Y-L, Zhao Y-Z, Zhao L, Li X, Chen H, Zhang L-F, et al. Experimental studies on temperature rise within a hydrogen cylinder during refueling. *Int J Hydrogen Energy* 2010;35:2627–32. <https://doi.org/10.1016/j.ijhydene.2009.04.042>.
- [3] Suryan A, Kim HD, Setoguchi T. Three dimensional numerical computations on the fast filling of a hydrogen tank under different conditions. *Int J Hydrogen Energy* 2012;37:7600–11. <https://doi.org/10.1016/j.ijhydene.2012.02.019>.
- [4] Bourgeois T, Ammouri F, Baraldi D, Moretto P. The temperature evolution in compressed gas filling processes: a review, vol. 43. Elsevier Ltd; 2018. <https://doi.org/10.1016/j.ijhydene.2017.11.068>.
- [5] Melideo D, Baraldi D, Acosta-Iborra B, Ortiz Cebolla R, Moretto P. CFD simulations of filling and emptying of hydrogen tanks. *Int J Hydrogen Energy* 2017;42:7304–13. <https://doi.org/10.1016/j.ijhydene.2016.05.262>.
- [6] Johnson T, Bozinoski R, Ye J, Sartor G, Zheng J, Yang J. Thermal model development and validation for rapid filling of high pressure hydrogen tanks. *Int J Hydrogen Energy* 2015;40:9803–14. <https://doi.org/10.1016/j.ijhydene.2015.05.157>.
- [7] Kim SC, Lee SH, Yoon KB. Thermal characteristics during hydrogen fueling process of type IV cylinder. *Int J Hydrogen Energy* 2010;35:6830–5. <https://doi.org/10.1016/j.ijhydene.2010.03.130>.
- [8] Kim SC, Lee SH, Yoon KB. Thermal characteristics during hydrogen fueling process of type IV cylinder. *Int J Hydrogen Energy* 2010;35:6830–5. <https://doi.org/10.1016/j.ijhydene.2010.03.130>.

- [9] De Miguel N, Acosta B, Baraldi D, Melideo R, Ortiz Cebolla R, Moretto P. The role of initial tank temperature on refuelling of on-board hydrogen tanks. *Int J Hydrogen Energy* 2016;41:8606–15. <https://doi.org/10.1016/j.ijhydene.2016.03.158>.
- [10] Molkov V, Dadashzadeh M, Makarov D. Physical model of onboard hydrogen storage tank thermal behaviour during fuelling. *Int J Hydrogen Energy* 2019;44:4374–84. <https://doi.org/10.1016/j.ijhydene.2018.12.115>.
- [11] Liu J, Zheng S, Zhang Z, Zheng J, Zhao Y. Numerical study on the fast filling of on-bus gaseous hydrogen storage cylinder. *Int J Hydrogen Energy* 2020;45:9241–51. <https://doi.org/10.1016/j.ijhydene.2020.01.033>.
- [12] Charolais A, Ammouri F, Vyazmina E, Nouvelot Q, Guewouo T, Greisel M, et al. Protocol for heavy-duty hydrogen refueling: a modelling benchmark. *International Conference on Hydrogen Safety*; 2021.
- [13] Dicken CJB, Mérida W. Modeling the transient temperature distribution within a hydrogen cylinder during refueling. *Null* 2007;53:685–708. <https://doi.org/10.1080/10407780701634383>.
- [14] Carrere P, Lodier G, Vyazmina E, Ammouri F, Charolais A, Gonin R. CFD simulations of the refueling of long horizontal H2 tanks. *Int Conf Hydr Saf* 2021.
- [15] Zou Q, Tian Y, Han F. Prediction of state property during hydrogen leaks from high-pressure hydrogen storage systems. *Int J Hydrogen Energy* 2019;44:22394–404. <https://doi.org/10.1016/j.ijhydene.2019.06.126>.
- [16] Johnston IA. The Noble-Abel equation of state: thermodynamic derivations for ballistics modelling. *Defence Science and Technology Organisation Edinburgh (Australia) Weapons Ststem Div*; 2005.